This relation may be regarded as a consequence of interpreting our barrier measurement, $B_f = 22.5 \pm 1.5$ MeV, in terms of the liquid-drop model. Another way of stating our result, which is independent of the assumption of this model, is that we have determined the mass of the Tl^{201} nucleus in that (saddle point) configuration where the cohesive and disruptive forces are just balanced in unstable equilibrium. This mass is equal to the ground-state mass of Tl^{201} (Ref. 14) plus 22.5 MeV, or $M_{\text{saddle point}}(Tl^{201}) = 200.9994 \pm 0.0015$ mass units on the carbon scale. An adequate semiempirical mass formula ought to reproduce this saddle-point mass as well as the ground-state masses of nuclei.

VI. CONCLUSIONS

A new method involving the detection of fission fragments in mica has been applied to the measurement of the fission cross section of the compound nucleus Tl^{201} produced by bombardments of Au^{197} with helium ions. These data have been interpreted in terms of an expression for Γ_f/Γ_n having four adjustable parameters which include a fission barrier thickness parameter $\hbar\omega$. The results are that the fission barrier of Tl^{201} is 22.5 ± 1.5 MeV and the value of $\hbar\omega$ is in the range 0.0 to about 2 MeV. The values of the level density parameters obtained are $a_f \approx 16$ and $a_n \approx 12$, with large uncertainties. The value of $(Z^2/A)_{\text{limiting}}$ calculated from the above-mentioned barrier estimate is 48.4 ± 0.5, which is within about a half-unit of the first estimate of Bohr and Wheeler.

ACKNOWLEDGMENTS

The work of adopting the least-squares fitting program to the theoretical functions, data fittings proper, and all activities directly concerned with the computers were carried out by Claudette Rugge. Her outstanding contribution to this work deserves the highest recognition.

We are grateful to Bernard G. Harvey and the staff of the 88-in. cyclotron for help and cooperation with the experimental work. We also acknowledge the valuable assistance of Jean Rees and Joan Phillips in preparing this manuscript and in helping with the scanning. We are grateful to Ray Nix and John Huizenga for very valuable discussions. We appreciate the support given by the General Electric Company in enabling one of us (Price) to take part in these experiments.

This work was done under the auspices of the U. S. Atomic Energy Commission.

PHYSICAL REVIEW VOLUME 134, NUMBER 5B 8 JUNE 1964

Excitation of the Giant Resonance in C^{12} and O^{16} by Inelastic Electron Scattering*

J. GOLDEMBERG† AND W. C. BARBER
High-Energy Physics Laboratory, Stanford University, Stanford, California
(Received 23 January 1964)

The excitation of the electric-dipole giant resonance in C^{12} and O^{16} was studied by measuring the spectrum of electrons inelastically scattered at 180°. Experiments were made with incident electrons of 40, 55, and 70 MeV; combining these data with the known photon absorption cross section a form factor for the giant resonance cross section is obtained for momentum transfers up to 120 MeV/c. The form factor for the combined strength of the main giant resonance in C^{12} and O^{16} which is concentrated between 20 and 25 MeV has a very characteristic shape going through a shallow minimum and increasing again with the momentum transfer. A comparison of the data with calculations of Lewis and Walecka using an extended shell model of the giant resonance indicates quantitative agreement, while collective models (such as the Goldhaber-Teller and Steinwedel-Jensen) fail to explain the data. The cross sections display also some fine structure. In C^{12} peaks are seen at 18.1, 19.5, 24, and 34 MeV; in O^{16} the peaks are at 19, 22.5, and 25.5 MeV.

I. INTRODUCTION

THE use of inelastic electron scattering to excite the giant resonance which is present in the interaction of photons with nuclei presents several advantages which have not yet been explored fully:

(a) The precise definition of the energy of the initial and scattered electrons determines the energy absorbed by the nucleus eliminating the difficulties present in the case of a continuous bremsstrahlung spectrum.

(b) The cross section for inelastic electron scattering gives direct information on the interaction mechanism of the electrons with the nucleus without the complication of measuring either residual activities or outgoing protons, neutrons, or other particles which compete in

* This study was based on work at Stanford University supported in part by the joint program of the Office of Naval Research and the Air Force Office of Scientific Research and on work at the Institut für Technische Kernphysik der Technischen Hochschule, Darmstadt, Germany.

† Present address: Departamento de Fisica, Universidade de São Paulo, Sao Paulo, Brazil.

determining the decay process. These particles can of course be measured and give further information on the decay processes of the highly excited states; we will not concern ourselves with this problem here.

(c) The momentum transferred to the nucleus can be varied independently of the energy transferred, and thus the spatial distribution of the nuclear electric-dipole operator can be inferred.

A general expression for inelastic electron scattering in Born approximation and with neglect of nuclear recoil and the electron mass (with respect to its energy) is[1,2]

$$\frac{d\sigma}{d\Omega}(J_f \leftarrow J_i)=\frac{k_2}{k_1}\frac{8\pi\alpha^2}{\Delta^4}\Big[V_L(\theta)\sum_{J=0}^{\infty}\frac{1}{2J_i+1} \times|\langle J_f||M_J(q)||J_i\rangle|^2+V_T(\theta)\sum_{J=1}^{\infty}\frac{1}{2J_i+1} \times(|\langle J_f||T_J^{\mathrm{el}}(q)||J_i\rangle|^2 +|\langle J_f||T_J^{\mathrm{mag}}(q)||J_i\rangle|^2)\Big], \quad (1)$$

where k_1 and k_2 are the initial and final electron wave numbers, $\mathbf{q}^2=(\mathbf{k}_2-\mathbf{k}_1)^2$ and $\Delta^2=\mathbf{q}^2-(k_2-k_1)^2$ are the 3- and 4-momentum transfers; θ is the electron scattering angle, and

$$V_L(\theta)=(\Delta^4/q^2)2k_1k_2\cos^2(\theta/2), \quad (2)$$

$$V_T(\theta)=(2k_1k_2/\Delta^2)\sin^2(\theta/2) \times[(k_1+k_2)^2-2k_ik_2\cos^2(\theta/2)]. \quad (3)$$

The multipole operators $M_J(q)$, $T_J^{\mathrm{el}}(q)$, and $T_J^{\mathrm{mag}}(q)$ contain the nuclear charge $e\rho_N(\mathbf{x})$, current $e\mathbf{j}_N(\mathbf{x})$, and magnetization $e\boldsymbol{\mu}_N(\mathbf{x})$ densities. The operators $T_J^{\mathrm{el}}(q)$ and $T_J^{\mathrm{mag}}(q)$ are exactly the same which describe the emission and absorption of photons in which case $\hbar c|\mathbf{q}_{\mathrm{ph}}|=\Delta E=E_{fi}$. The quantities J_i and J_f are the spins of the initial and final states involved. The coefficients of $V_L(\theta)$ and $V_T(\theta)$ are called, respectively, the longitudinal and transverse matrix elements squared, and the inelastic cross section can accordingly be broken up in two terms.

$$\frac{d\sigma}{d\Omega}(J_f \leftarrow J_i)=\left(\frac{d\sigma}{d\Omega}\right)_L+\left(\frac{d\sigma}{d\Omega}\right)_T. \quad (4)$$

The nature of the difficulties involved in using electron scattering in the studies of the giant resonance has been discussed before in some detail.[3] We will summarize here the main conclusions of the discussion:

(a) If one measures the inelastic scattering cross sections at small and intermediate angles ($\theta<150°$), the cross section is dominated by the longitudinal part; the ratio of this cross section to the elastic scattering cross section is small for small momentum transfers and increases with q^2. Experiments using this technique have been reported recently for O^{16} by Isabelle and Bishop.[4]

(b) If the measurements are made at very large angles ($\theta\sim180°$) the scattering is dominated by the transverse terms and the ratio to the elastic electron scattering is independent of the momentum transfer, and becomes very large as $\theta\rightarrow180°$.

All the Stanford work reported in this paper was done at 180°, some preliminary experiments were done with an incident electron energy of 40 MeV,[3] afterwards the energy was increased to[5] 55 and then to 75 MeV. The importance of using energies higher than 40 MeV will be apparent later. Measurements were made for C^{12} and O^{16}. At Darmstadt measurements were made at 128° and 152° to explore a limited region of the C^{12} spectrum with high resolution.

In Sec. II we describe some experimental problems; in Sec. III we present the results; in Sec. IV we compare them with theory and in Sec. V some conclusions are listed.

II. EXPERIMENTAL DETAILS

The equipment used in 180° scattering experiments at the Stanford Mark II Accelerator was described previously.[3,6] In the target area an analyzed beam of electrons from the accelerator is deflected approximately 10° by a small auxiliary magnet before striking a target and the electrons that are scattered in the backward direction are deflected again another 10° in the same magnet and then enter a magnetic spectrometer where they are analyzed and detected by a telescope of scintillation counters.

The Mark II accelerator was modified for the present experiments in order to accelerate electrons up to an energy of 75 MeV. Two 10-ft sections of constant gradient design were installed together with two klystrons. Other minor improvements in the accelerator were also made but they will not be described here.

The main problem in the measurements is the continuous "radiation tail" that forms a background under the inelastic peaks. Although the Mott cross section goes to zero at 180°, multiple scattering and the finite aperture of the spectrometer mean that there is always a residual elastic peak from electrons scattered at large angles such as 178°. This elastic peak has an associated "radiation tail."

The background effects become smaller at higher energies. The elastic cross sections go down inversely

[1] L. I. Schiff, Phys. Rev. **96**, 765 (1954).
[2] J. D. Walecka, Phys. Rev. **126**, 653 (1962).
[3] J. Goldemberg, Y. Torizuka, W. C. Barber, and J. D. Walecka, Nucl. Phys. **43**, 242 (1963).
[4] D. B. Isabelle and G. R. Bishop, Nucl. Phys. **45**, 209 (1963).
[5] F. H. Lewis, Jr., J. D. Walecka, J. Goldemberg, and W. C. Barber, Phys. Rev. Letters **10**, 493 (1963).
[6] G. A. Peterson and W. C. Barber, Phys. Rev. **128**, 812 (1962).

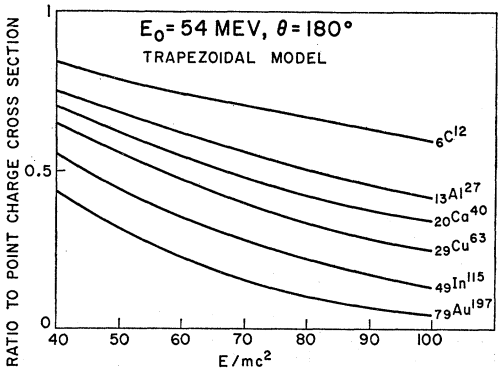

FIG. 1. Curves showing the effect of the finite extent of the nucleus on the bremsstrahlung cross section. The ordinate gives the ratio of the corrected cross section to the point nucleus cross section, Eq. (5).

proportional to the energy squared. The bremsstrahlung cross section from a point nucleus where the electron is scattered at 180° and the photons are radiated at any angle is given by[7]

$$\left(\frac{d\sigma}{d\Omega}\right)_b=\frac{\alpha Z^2}{8\pi}r_0^2\frac{m_0^2c^4}{(\hbar k_1 c)^3}(1-\gamma-\gamma^{-1}+\gamma^{-2}), \quad (5)$$

where $\gamma=k_2/k_1$.

It is seen that for a given γ this cross section decreases as the third power of the incident energy. Furthermore, since the giant resonance is 20 MeV below the elastic peak, $\gamma\rightarrow 1$ as k_1 increases and consequently $(d\sigma/d\Omega)_b\rightarrow 0$.

Furthermore one has to consider the fact that finite nuclear size effects in bremsstrahlung become appreciable at the momentum transfers involved. These effects were calculated in detail by Ginsberg and Pratt.[8] The bremsstrahlung cross section is smaller than that given in Eq. (5) by an amount that depends on the energy loss, i.e., γ. Figure 1 shows the results for an incident energy of 54 MeV as given in the form of a ratio to the point charge cross section, Eq. (5).

As it will be seen later, the reduced matrix elements for the excitation of the giant resonance increase with the momentum transfer. As a result the inelastically scattered electrons stand up more clearly at higher incident energies. The trend probably continues (at 180°) up to energies of 200 MeV but at these energies incoherent scattering by the individual nucleons (quasi-elastic scattering) becomes important and makes the interpretation of the experiments more complicated.

III. RESULTS

Measurements were made in C^{12} using a pure graphite target 408 mg/cm² thick (0.009 radiation length). For O^{16} distilled water contained between two very thin Mylar films was used. The thickness of the water was $\frac{1}{8}$ in. (0.01 radiation length).

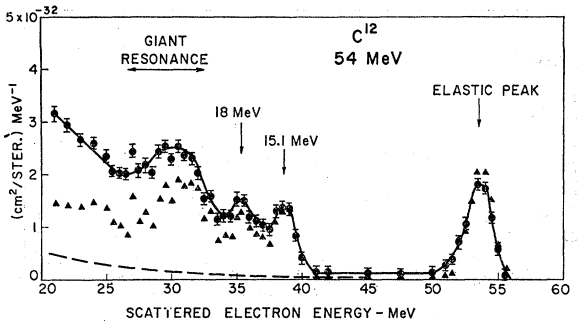

FIG. 2. Spectrum of electrons, initially 54 MeV, scattered at 180° from a graphite target.

Figure 2 shows the spectrum of electrons inelastically scattered from carbon with 54-MeV incident electrons. The raw data were corrected for radiative effects[9] using an iterative procedure setup for a 7090-IBM computer.[10] These radiative effects remove electrons from a given energy and spread them down in a spectrum of lower energies. The computer calculation begins by dividing the spectrum in bins of width ΔE. The cross section in the highest energy bin is then multiplied by a factor e^{δ} that corrects for the electrons radiated out of that bin.

$$\left(\frac{d\sigma}{d\Omega}\right)_{\text{real}}=\left(\frac{d\sigma}{d\Omega}\right)_{\text{observed}}e^{\delta(\Delta E)}, \quad (6)$$

$$\delta=\frac{2\alpha}{\pi}\left\{\left[\tfrac{1}{2}\ln\left(\frac{E_0}{\eta^2\Delta E}\right)+\tfrac{1}{2}\ln\left(\frac{E_0}{\Delta E}\right)-\frac{13}{12}\right]\times\left[2\ln\left(\frac{q^2}{m^2}\right)-1\right]+\frac{17}{36}\right\}, \quad (7)$$

α = fine structure constant, M = nucleon mass, A = mass number, $\eta=1+[2E_0\sin^2(\theta/2)/MAc^2]$.

The cross section of the second bin ΔE MeV below the first is then reduced by the amount that comes from

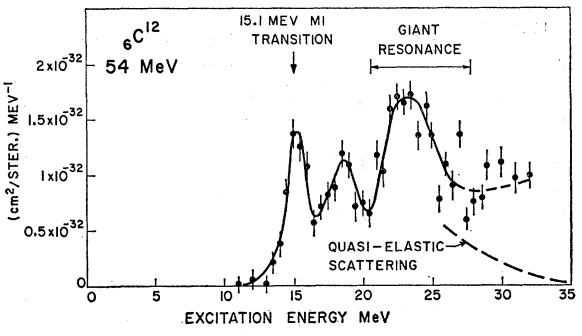

FIG. 3. Cross section for inelastic scattering from carbon derived from the spectrum shown in Fig. 2.

[7] P. T. McCormick, D. G. Keiffer, and G. Parzen, Phys. Rev. **103**, 29 (1956).
[8] E. Ginsberg and R. H. Pratt (private communication).
[9] Y. S. Tsai, Phys. Rev. **122**, 1898 (1961).
[10] H. Crannell (private communication).

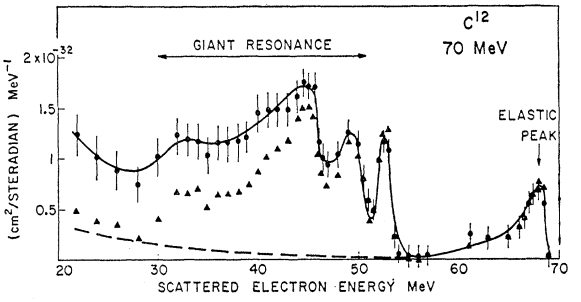

FIG. 4. Spectrum of electrons, initially 70 MeV, after scattering 180° from a graphite target.

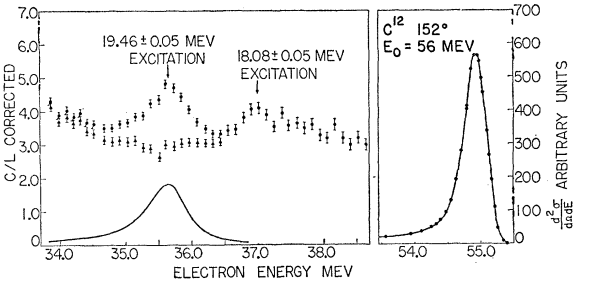

FIG. 6. Spectrum of electrons, scattered from C with excitation energy in the region of 19 MeV. The inelastic cross section for the excitation of the peak at 19.46 MeV was derived by comparison with the elastic peak, shown at the right, measured using the same target and spectrometer angle.

electrons that would have been at higher energies had there been no radiation and then multiplied by its own e^{δ} factor to correct for the electrons that were removed from it. A reduced energy electron can be produced by radiation either before or after scattering and in the former case the scattering probability is enhanced by the factor $E_0^2F^2(q^2)/E^2F^2(q_0)$ (q_0 corresponding to E_0 and q corresponding to E). Because of this, the program applies a correction of $\frac{1}{2}\{1+(E_0^2/E^2)[F^2(q)/F^2(q_0)]\}$ at the appropriate place as the iterative process described above is carried out. This correction does not have a large effect because the probability of multiple emission of soft photons becomes very small as E becomes much less than E_0.

The applications of these corrections gives the triangular points of Fig. 2. In addition it is necessary to subtract the bremsstrahlung cross section (after finite size effects have been considered). This cross section is given by the dashed line in Fig. 2.

The final result for the cross section plotted as a function of excitation energy is shown in Fig. 3. The lowest energy peak is the 15.1-MeV level which comes from the reduced matrix element $\langle 1^+||T_J^{\rm mag}(q)||0^+\rangle$ in Eq. (1). The remaining cross section is attributed to the excitation of the giant resonance. A peak is seen at 18.7 MeV and a broad resonance at ~24 MeV. A 34-MeV level, which is part of the family of levels responsible for the giant resonance, according to the shell model[5] was not observed in the 54-MeV experiments because the low residual energy of the electron made it difficult to explore this region of the inelastic spectrum.

Figure 3 shows as a dashed line an estimate of the contribution of the quasielastic scattering to our cross section.

Figure 4 shows data taken on the same carbon target at 70 MeV where the same treatment of the experimental data was applied. Figure 5 shows the cross sections derived from Fig. 4 which displays clearly the peaks at 15.1, 18.7, 24, and 35 MeV. Also shown in this figure are the photon absorption measurements of Bezic *et al.*[11]

The relative importance of the peak at 18.7 MeV is growing rapidly with increasing momentum transfer. This behavior was previously observed by Leiss and Taylor,[12] and because of this they thought multipoles higher than dipole were making a contribution. We shall show that the momentum transfer dependence of this peak is consistent with an electric-dipole transition. There is also a broad state in C^{12} centered at about 17.2 MeV that is listed by Ajzenberg-Selove and Lauritsen[13] as a 1^- $T=1$ state. This state does not appear in the Stanford experiments, perhaps because of

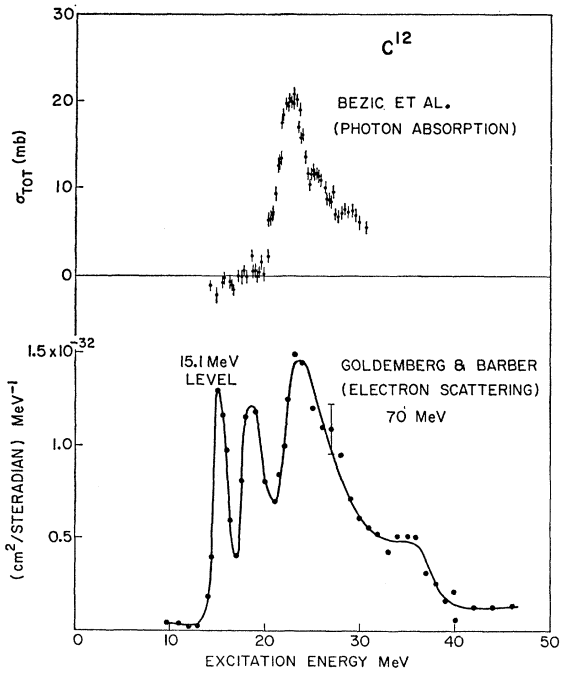

FIG. 5. The lower curve shows the cross section for inelastic scattering from C derived from the spectrum shown in Fig. 4. The upper curve shows for comparison the total cross section for photon absorption by the C nucleus.

[11] N. Bezic, D. Jamnik, G. Kernel, and J. Snajder (private communication).

[12] J. E. Leiss and R. E. Taylor, Karlsruhe Photonuclear Conference, 1960 (unpublished).

[13] F. Ajzenberg-Selove and T. Lauritsen, Nucl. Phys. **11**, 1 (1959).

TABLE I. Parameters of the lowest dipole state in C^{12} calculated by F. H. Lewis, Jr. (Ref. 20) for the conditions of the Darmstadt experiments. The symbols are the same as those appearing in Eq. (1).

E_0 (MeV)	θ deg	q Inel. (MeV/c)	$V_L(\theta)$ (MeV/c)^2	$V_T(\theta)$ (MeV/c)^2	$\lvert\langle 1^-\rvert\rvert M_1(q)\rvert\rvert 0^+\rangle\rvert^2$	$\lvert\langle 1^-\rvert\rvert T_1^{el}(q)\rvert\rvert 0^+\rangle\rvert^2$	$(d\sigma/d\Omega)\times 10^{32}$ (cm^2/sr)
56	152	90	220	4000	0.00134	0.00067	1.68
50	152	77	160	3000	0.00123	0.00057	1.93
40	152	59	80	1600	0.00090	0.00043	2.09
55	128	81	700	3500	0.00129	0.00062	2.58

the relatively poor energy resolution. In order to study this region of the spectrum in more detail one of us (WCB) made measurements using the linear electron accelerator and the scattering apparatus of the Institut für Technische Kernphysik der Technischen Hochschule Darmstadt. This apparatus permits high resolution measurements at scattering angles up to 165°. A detailed description of the apparatus and some electron scattering results have been given by Gudden *et al.*[14]

The region of 16–20-MeV excitation in C^{12} was explored at four different combinations of energy and angle. A peak was observed at about 19.5-MeV excitation in all four cases, but it was most prominent at the highest momentum transfer, 56-MeV primary electrons scattered at 152°. This result is shown in Fig. 6. Also shown on Fig. 6 are the elastic peak and a small peak at 18.1 MeV. The 19.5-MeV peak was analyzed by folding the expected resolution curve at 19.5-MeV with a resonance curve having a width of 0.5-MeV. The resulting curve is shown at the bottom left of Fig. 6. If this curve is centered at 19.46-MeV and subtracted from the experimental points, the points indicated by solid triangles are the result. Preliminary attempts to calculate the continuous background of the spectra observed with the Darmstadt apparatus were not successful, but the triangles show the expected dish-shaped behavior if there were no nuclear states in the neighborhood of 19.5 MeV. On the left the points are rising to the main giant resonance and on the right to the 18.1-MeV peak. The fit is satisfactory and the estimated error in assigning the area of the 19.5-MeV peak relative to the elastic peak is $\pm 10\%$. The observed peak width of (0.61 ± 0.06) MeV is made up of (0.34 ± 0.03) MeV for resolution and (0.5 ± 0.1) MeV for nuclear width.

The small peak at 18.1 MeV appears to be the highest point of a broad peak or a succession of levels extending on down to an excitation energy of less than 17 MeV. It thus includes the region of the 17.2-MeV 1^- state which is reported to have a width of about 1.2 MeV. Because of the difficulty in assigning a background under such a broad peak it is impossible to assign an accurate value to the peak area. We estimate it to have 80% of the 19.5-MeV peak with an estimated error of $+50\%$ and -30%.

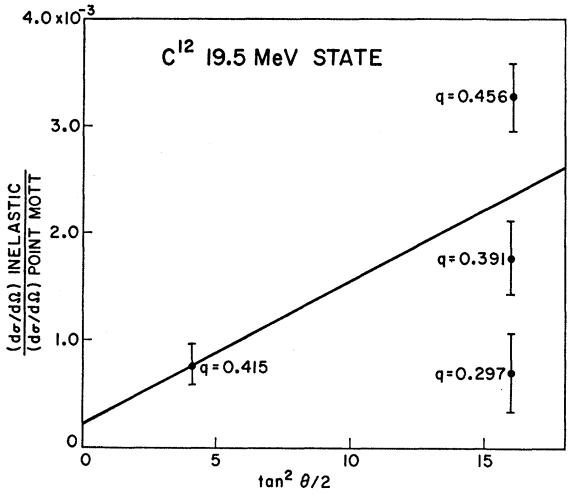

FIG. 7. Ratio of the experimental inelastic cross section to the Mott cross section plotted as a function of the tangent squared of one-half the scattering angle. On this plot points measured at constant q should fall on a straight line whose slope is proportional to the coefficient of V_T in Eq. (1).

The results for both peaks for the four different measurements are summarized in Table I and Table II. The data on the 19.5-MeV peak are plotted in Fig. 7. Figure 7 has as ordinate the ratio of the inelastic cross

TABLE II. Cross sections for excitation of the 18.1- and 19.5-MeV states observed in the Darmstadt carbon scattering experiments.

E_0 (MeV)	deg	$(d\sigma/d\Omega)\times 10^{32}$ (19.5-MeV state)	$(d\sigma/d\Omega)\times 10^{32}$ (18.1-MeV state)	$(d\sigma/d\Omega)\times 10^{32}$ (Both states)	$\lvert\langle 1^-\rvert\rvert T_1^{el}(q)\rvert\rvert 0^+\rangle\rvert^2$ (19.5-MeV state only)	$\lvert\langle 1^-\rvert\rvert T_1^{el}(q)\rvert\rvert 0^+\rangle\rvert^2$ (Both states)
56	152	1.3 ± 0.13	$1.0\pm_{0.3}^{0.5}$	$2.3\pm_{0.3}^{0.5}$	0.00053 ± 0.00005	$0.00091_{-0.00012}^{+0.00020}$
50	152	0.88 ± 0.18	1.0 ± 0.2	1.9 ± 0.3	0.00026 ± 0.00005	0.00057 ± 0.00009
40	152	0.55 ± 0.3	0.5 ± 0.4	1.1 ± 0.5	0.00012 ± 0.00007	0.00023 ± 0.00011
55	128	1.4 ± 0.3	0.5 ± 0.4	1.9 ± 0.5	0.00034 ± 0.00007	0.00046 ± 0.00012

[14] F. Gudden, G. Fricke, H. G. Clerc, and P. Brix (unpublished).

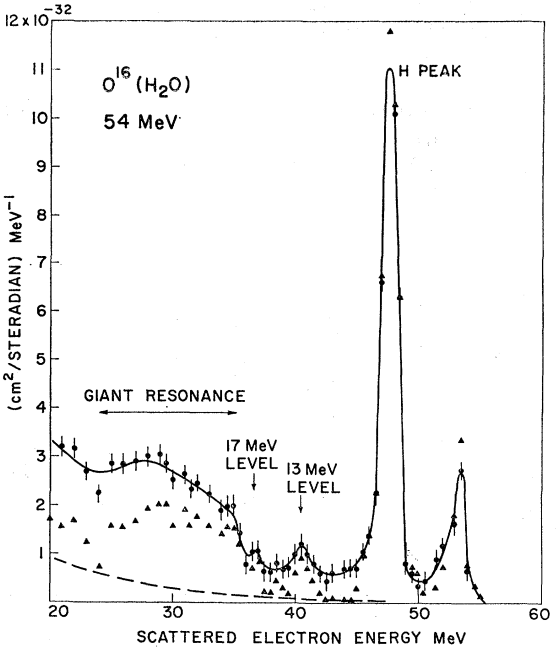

FIG. 8. Spectrum of electrons, initially 54 MeV, after scattering at 180° from a water target.

section to the Mott cross section for the scattering from a point nucleus. This ratio is determined from the experimental ratio of the area of inelastic and elastic peaks together with known values of the elastic form factor of the carbon nucleus. We plot as abscissa $\tan^2\theta/2$ because in such a plot, points of constant q should lie on a straight line whose slope is proportional to the transverse part of the inelastic cross section. The four points were taken at different values of momentum transfer, but it is clear from their locations that the transverse part of the cross section is dominant in the 152° experiments.

In Fig. 8 we show the results for O^{16} at 54 MeV. Figure 9 shows similar results for 70 MeV. In Fig. 10 we show the inelastic electron scattering cross section in O^{16} at 70 MeV together with the photon absorption measurements of Burgov *et al.*[15]

IV. DISCUSSION

Figure 11 shows as points the reduced matrix element $|\langle 1^-|T_1^{el}(q)||0^+\rangle|^2$ calculated using Eq. (1) and the measured integrated cross section in carbon in the region between 20 and 26 MeV. The point at a momentum transfer of 60 MeV/c was taken from a previous paper.[3] The point at the lowest momentum transfer was obtained from the integrated cross section over the giant resonance for the dominant processes (γ,n) and (γ,p) using data available in the literature as summarized by Hayward.[16] The reduced matrix element in this case was obtained using the equation

$$\int \sigma_{\rm abs}(E)dE = (2\pi)^3\alpha \frac{(\hbar c)^2}{E_{fi}} \frac{1}{2J_i+1} \times \sum_J |\langle J_f|\left|T_J^{el}\left(\frac{E_{fi}}{\hbar c}\right)\right||J_i\rangle|^2, \quad (8)$$

which is given by Lewis and Walecka.[17]

Also shown in Fig. 11 are three curves, results of the calculations of Lewis and Walecka[17] using shell-model wave functions taking into account the mixing of the possible particle-hole configurations (Brown model). In this model as shown by Lewis and Walecka each of the levels that contribute to the giant resonance has its own form factor which can be quite different from those of the other levels present as far as q dependence is concerned. The calculation predicts four levels at energies of 19.6, 23.3, 25.0, and 35.8 MeV. Consequently the shape of the giant resonance (which is defined as the envelope of the cross section made up of the contribution of the levels) will change as the momentum transfer increases. The lowest level is relatively unimportant at low momentum transfer but is predicted to grow rapidly with momentum transfer. For some other levels the form factor decreases with increasing momentum transfer. In drawing the three theoretical lines in Fig. 11, the sum of the two levels that contribute in the region between 20 and 26 MeV in carbon was considered. The three curves are for three slightly different cases.

The solid line assumed a zero-range spin-dependent two-particle interaction, the long-dash–short-dash curve a Serber force with a Yukawa well shape. The dashed curve was from a calculation where the highest energy unperturbed state was left out of the calculation. In

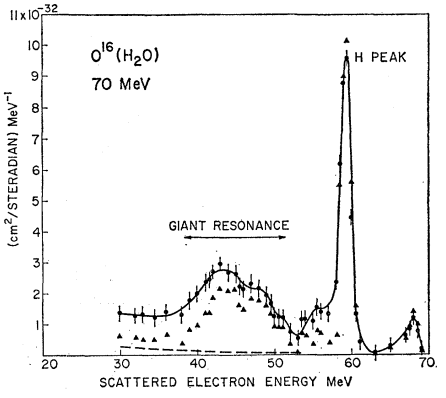

FIG. 9. Spectrum of electrons, initially 70 MeV, after scattering at 180° from a water target.

[15] N. A. Burgov, G. V. Danilyan, B. S. Dolbilkin, L. E. Lazareva, and F. A. Nikolaev, Zh. Eksperim. i Teor. Fiz. **43**, 70 (1962) [English transl.: Soviet Phys.—JETP **16**, 50 (1963)].

[16] E. Hayward, Rev. Mod. Phys. **35**, 324 (1963).

[17] F. H. Lewis, Jr., and J. D. Walecka, Phys. Rev. **133**, B849 (1964).

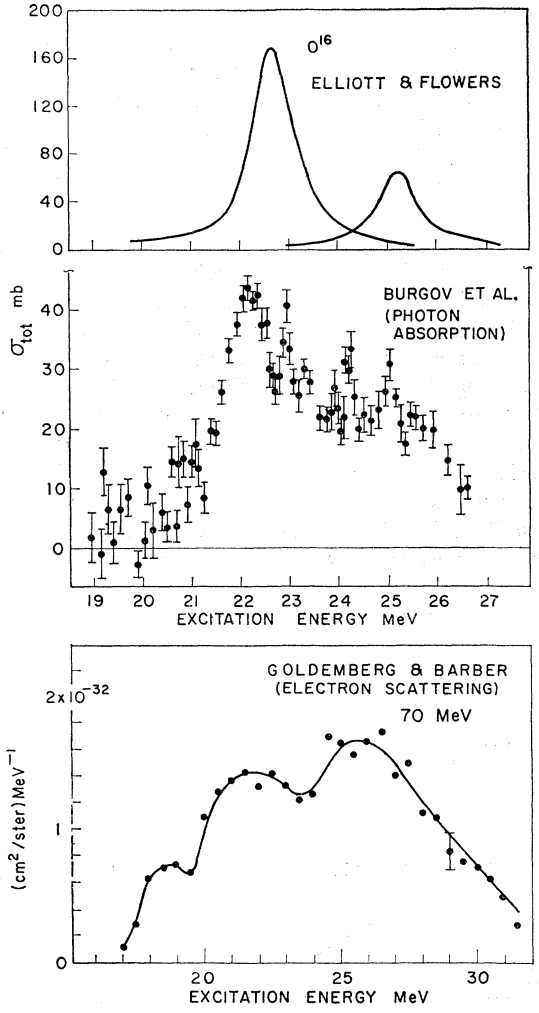

FIG. 10. The lower curve shows the cross section for inelastic scattering from oxygen derived from the spectrum shown in Fig. 9. The middle curve shows for comparison the total cross section for photon absorption by the oxygen nucleus. The upper curve shows the cross section for photon absorption in the region of the giant resonance as calculated by Elliott and Flowers.

this case there are only three states but two of them are between 20 and 26 MeV and the result for this region is about the same. The most outstanding features of all of the shell-model form factors of Fig. 11 are the initial decrease with q, a shallow minimum followed by a steady increase over an interval of approximately 100 MeV/c. The data obtained in this experiment are in good agreement with these predictions. Figure 11 contains also the predictions of the Goldhaber-Teller[18] and Steinwedel-Jensen[19] models of the giant resonance, and as it can be seen the form factor decreases monotonically for large momentum transfers in complete variance with experiment. The absolute values of the form factors in this case are approximately a factor of 2 larger than experiment. One reason for that is the fact that in these collective models all the transition strength is concentrated between 20 and 26 MeV. Experimentally we considered only the contribution in this region. The calculations of Lewis and Walecka predict only two out of a total of four levels to be in this region.

The predicted form factors for the lowest level in C^{12} are shown by the solid curves in Fig. 12. In comparing these with experiment we are faced with the difficulty that the high resolution experiments display at least two levels in this region. One possible interpretation is that there are two or more dipole states in this region, and that the theory is not developed in sufficient detail to display all of the structure. In this case it is possible that the theoretical calculation for the transition strength should apply to the sum of the states. The experimental data from the 180° experiments does not resolve the peaks. The single peak observed at 18.7 MeV in the 180° experiments is just between the 19.5- and 18.1-MeV peaks of Fig. 6, and therefore it is a good assumption that the 180° data include contributions from both peaks. The Darmstadt data were not taken at 180° and therefore include contributions of the longitudinal matrix elements to the cross section. From Fig. 7, however, it is plain that the transverse components are making the dominant contribution. This is in agreement with calculations of Lewis.[20] We have, therefore, used the results of Lewis to obtain a value for the ratio of the longitudinal to transverse contribution, and we have corrected the Darmstadt results accordingly to arrive at estimates of the transverse matrix elements only. These are given in Table II. These

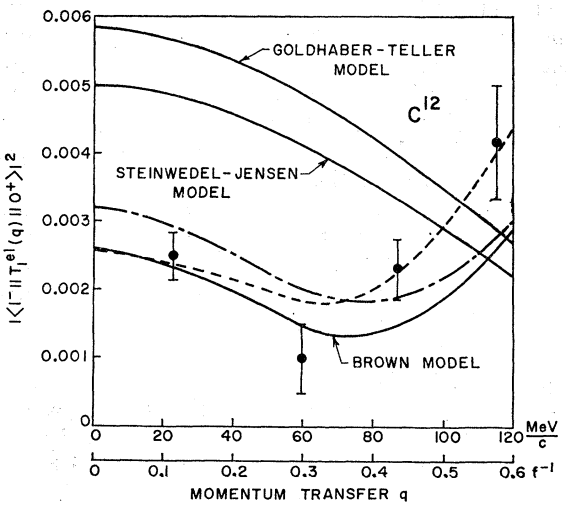

FIG. 11. The square of the form factor for the main part of the C^{12} giant resonance plotted as a function of momentum transfer. The experimental point at 23 MeV is from work with photons. The other three experimental points are from 180° electron scattering experiments. The curves are calculated on the basis of different theories as explained in the text.

[18] M. Goldhaber and E. Teller, Phys. Rev. 74, 1046 (1948).
[19] H. Steinwedel and J. H. D. Jensen, Z. Naturforsch. 59, 413 (1950).
[20] F. H. Lewis, Jr. (private communication).

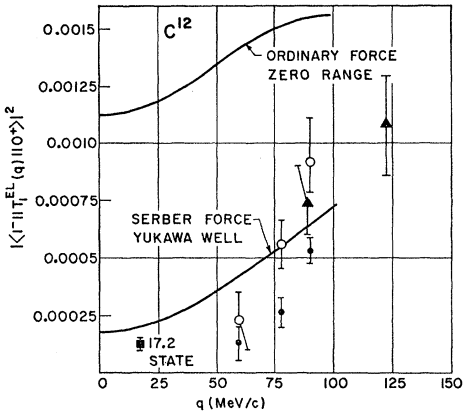

FIG. 12. Square of the form factor for the lowest 1^- state in C^{12} plotted as a function of the momentum transfer. The two curves are from the shell-model calculation for two different assumptions about the two-particle interaction. The triangles are from the Stanford 180° scattering experiments. The circles are from the Darmstadt 152° scattering experiments. The solid circles are for the single peak at 19.5 MeV whereas the open circles include the broad 18-MeV peak as well. The square is derived by detailed balancing from $B^{11}(p,\gamma)$ experiments which indicate a 1^- level at 17.2 MeV.

data are plotted on Fig. 12 for the 19.5-MeV state alone and for the sum of the 19.5- and 18.1-MeV states. Also shown on Fig. 12 are curves calculated by Lewis and Walecka for the matrix element of the lowest dipole state in C^{12} under two different assumptions about the nucleon-nucleon force. The experimental results for the sum of the 18.1- and 19.5-MeV levels are in agreement with the calculations using a Serber force, but if only one of the states is used the experimental values are about a factor of 2 too low. This in addition to the fact that the 19.5-MeV state is responsible for most of the strong increase with increasing q predicted by the theory, gives support to the supposition that the 19.5-MeV state is indeed a dipole state. We would like to emphasize, however, that there is no direct experimental proof of this and to suggest that further $B^{11}(p,\gamma)$ experiments might resolve this problem.

In Fig. 13 we show the reduced matrix elements for O^{16} corresponding to the excitation of the dominant levels at 22.5 and 25.5 MeV. Also shown are the calculations of Lewis[21] and again the same features outlined above for C^{12} are apparent here.

The Elliot and Flowers[22] calculation, shown at the top of Fig. 10, is made for photon absorption corresponding to experiments such as that of Burgov *et al.* shown in the center of Fig. 10. Experiment and theory are in agreement that the peak at about 22.5 MeV is considerably larger than the peak at 25.5 MeV. In the 70-MeV electron scattering experiments the situation is reversed. The 25.5-MeV peak is now larger than the lower energy one, just as the calculations of Lewis predict. Even though the independent particle-model calculations agree with experiment in considerable detail, the case of O^{16} shows up some deficiencies in the theory. The number of states observed experimentally is considerably higher than the number 5 predicted by the model. The central graph of Fig. 10 indicates four or more states in the region where the theory gives only two. The existence of this fine structure in O^{16} giant resonance is confirmed by high resolution $O^{16}(\gamma,p)$, $O^{16}(\gamma,n)$ and $N^{15}(p,\gamma)$ results which have been summarized by Finckh *et al.*[23] This extra fine structure which was also noted in the 17–20-MeV region of C^{12} does not mean that the theory is wrong. It is correct in predicting the over-all strength and distribution of the $E1$ states. The explanation of the additional structure is probably to be explained by the mixing of states not considered in the present calculation with the dominant dipole states.

In Figs. 8 and 9 one can see also some structure in the region where known 1^- levels have been found in

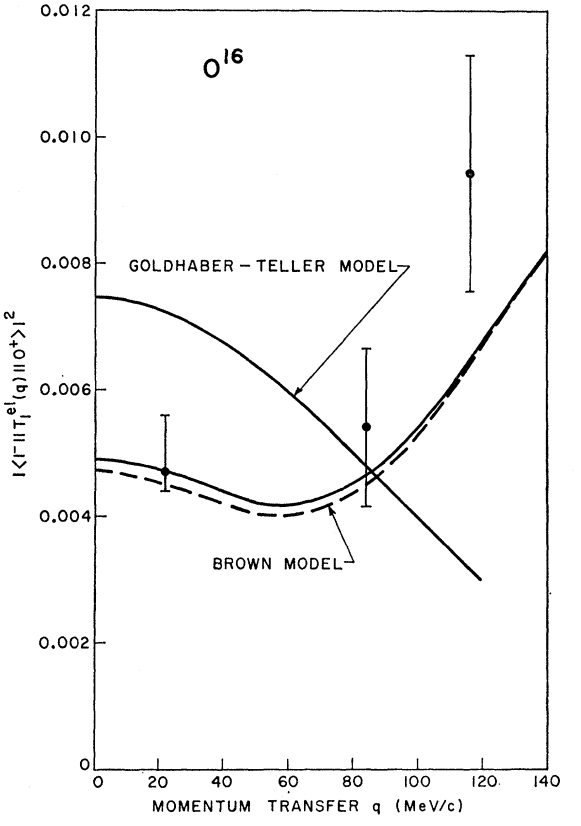

FIG. 13. The square of the form factor for the main part of the O^{16} giant resonance plotted as a function of momentum transfer. The experimental point at 23 MeV is from work with photons. The other three experimental points are from 180° electron scattering experiments. The curves are calculated on the basis of different theories as explained in the text.

[21] F. H. Lewis, Jr., Phys. Rev. **134**, B33 (1964).
[22] J. P. Elliott and B. H. Flowers, Proc. Roy. Soc. (London) **A242**, 57 (1957).
[23] E. Finckh, R. Kosiek, K. H. Lindenberger, K. Maier, U. Meyer-Berkhout, M. Schechter, and J. Zimmerer, Z. Physik **174**, 337–350 (1963).

the inverse reaction, $N^{15}(p,\gamma)O^{16}$. We will not present a detailed analysis of these levels because their cross section is rather small. Furthermore, they fall in a region where the elastic hydrogen peak appears; since the hydrogen peak is very large, it and its associated radiative tail mask the inelastic peaks.

V. CONCLUSIONS

The experiments described in this paper show that the modern shell model of the nuclei C^{12} and O^{16} succeeds in describing the dipole states of these nuclei in a detail far surpassing that of earlier models where the dipole resonance was explained as an oscillation of the protons against the neutrons. The resolution of experiments has, however, already progressed to the point of disclosing more levels than the theory predicts. We believe that improvements in the resolution and the accuracy of the experiments together with measurements over an increased range of momentum transfers will provide very fine discrimination in testing various description of nuclear states.

The experiments can be extended to investigate the giant resonance in other nuclei. We can obtain an estimate of the order of magnitude of the cross sections to be expected in heavier nuclei by using the Goldhaber-Teller model to calculate ratios of the transverse and longitudinal inelastic cross sections[3] to the Mott cross section. These ratios are an indication of the feasibility of measuring the giant resonance in the presence of the radiation tail of the elastic peak.

For the transverse part of the cross section we obtain

$$\left(\frac{d\sigma}{d\Omega}\right)_T \Big/ \left(\frac{d\sigma}{d\Omega}\right)_{\text{Mott}} = \frac{1}{2}\left(\frac{N}{A}\right)^2 \frac{\hbar\omega}{\mu c^2} \frac{1+\sin^2\theta/2}{\cos^2\theta/2}, \quad (9)$$

where $\mu=(AM)/4$. For a given θ this ratio is inversely proportional to A which makes experiments with heavy nuclei difficult. However, if enough intensity were available, the angular aperture of the spectrometer could be reduced to make θ effectively closer to 180° than at present (the angular acceptance of the 180° apparatus used in this experiment was about 2°).

For the longitudinal cross section, we obtain

$$\left(\frac{d\sigma}{d\Omega}\right)_L \Big/ \left(\frac{d\sigma}{d\Omega}\right)_{\text{Mott}} = \left(\frac{N}{A}\right)^2 \left(\frac{\hbar^2 q^2}{2\mu}\right)\left(\frac{1}{\hbar\omega}\right). \quad (10)$$

The ratio is again inversely proportional to A, but independent of angle, and proportional to q^2. The longitudinal part of the giant resonance shows up best in experiments at high values of momentum transfer.

ACKNOWLEDGMENT

One of us (WCB) wishes to thank Professor P. Brix and other members of the Darmstadt Technische Hochschule for their hospitality and support which made a part of this research possible.